ISSN 0018-151X, High Temperature, 2017, Vol. 55, No. 3, pp. 407–413. © Pleiades Publishing, Ltd., 2017.
Original Russian Text © I.V. Morenko, V.L. Fedyaev, 2017, published in Teplofizika Vysokikh Temperatur, 2017, Vol. 55, No. 3, pp. 426–432.

HEAT AND MASS TRANSFER AND PHYSICAL GASDYNAMICS

Nonisothermal Cross-Flow around a Cylinder with a Square Cross Section and an Impermeable Core Covered with a Porous Layer

I. V. Morenko[a, *] and V. L. Fedyaev[a, b]

[a] *Institute of Mechanics and Engineering, Kazan Science Center, Russian Academy of Sciences, Kazan, 420111 Russia*
[b] *Kazan National Research Technical University, Kazan, 420111 Russia*
**e-mail: morenko@imm.knc.ru*

Received March 6, 2015

Abstract—Nonisothermal cross flow of a viscous incompressible fluid around a porous cylinder with a square cross section is considered. Main attention is paid when an impermeable core of the cylinder is surrounded with a porous layer. The full system of Navier–Stokes and energy equations is integrated numerically by the finite-volume method. The hydrodynamic interaction between the flow and the matrix of the porous layer is described by Darcy's law. At moderate Reynolds numbers, the influence of the permeability of the porous layer on the nature of the flow and the heat exchange between the cylinder and the flow is studied. It is shown that, with increasing permeability, heat transfer from the cylinder increases mainly on its front side. From the analysis of the data obtained, an approximate formula for the mean Nusselt number as a function of the Reynolds and Darcy numbers is derived. The results of the calculation of hydrodynamic and thermal characteristics of the cross-flow around an impermeable and a fully permeable cylinder are also presented.

DOI: 10.1134/S0018151X17030154

INTRODUCTION

Bodies consisting of an impermeable core covered with one or several porous layers widely occur in nature and practice. The typical sizes of biological objects vary from fractions of a millimeter to dozens of meters. Those are cells of plants; viruses; microorganisms, in particular, bacteria; infusoria; mold; fungi; plants (including aquatic); insects; fish; shellfish; birds; and terrestrial animals with hair. In liquid and gaseous media, coating provides movement by means of cilia, the capture and propulsion of food, and the reduction in the aerohydrodynamic drag of birds and fish. The porous surfaces of the wings of birds and the tails and fins of fish enable them to fly, swim, and maneuver efficiently. Since porous permeable layers have a well-developed surface, their contact with the ambient medium intensifies nutritive and mass-exchange processes. However, the permeability of crowns of trees reduces the hydrodynamic drag and mechanical loads on the trunk and root system. The main purpose of hair is to protect the body of an animal from a mechanical action, e.g., flying sand, specula, acanthi, chemically aggressive media, radiation, and temperature loads. Human clothes and special protective devices perform similar functions [1–4].

Among technical objects comprising an impermeable core and a porous coating, it is worth distinguishing recuperating and regenerative heat exchangers [5]. Porous layers, in particular, in the form of finning, provide the development of the surface of walls separating heat carriers, enhance their heat transfer, and increase the heat capacity of a structure. At the same time, porous materials with a low thermal conductivity are widely used in various structures for heat insulation of industrial and residential buildings, heating networks, furnaces, boiler plants, refrigerators, etc. [6–9]. In the cases of high thermal loads, e.g., upon sheets of air- and spacecraft and elements of rocket engines, porous cooling systems are applied [10]. In this case, through a porous layer, a coolant is delivered to the incident flow. As is known, the efficiency of porous cooling is higher than those of convective, film, and barrier cooling. In addition, the injected gas reduces the friction drag of the streamlined surface.

The more complex structure of the composite objects as compared to the homogeneous necessitates additional description of the motion and heat transfer of fluid in a porous layer. In addition, the nature of the astern flow is complicated and the flow detachment point is displaced. Due to practical significance, problems of flow around bodies having a porous coating with heat exchange are of significant interest.

An isothermal flow in a channel of a square cross section with a porous layer was studied numerically in [11]. The Reynolds number $\mathrm{Re} = ua/\nu$ was determined from the edge length a of the cross section of the cylinder, the flow velocity u far from the streamlined body, and the kinematic viscosity ν of the fluid. For Reynolds numbers $\mathrm{Re} = 100$ and 200, the drag and lift of the cylinder were found. The thickness of the porous layer was 10, 15, and 20% of the edge length of the cylinder; the porosity κ was 0.4, 0.6, and 0.8; and

the Darcy number $\mathrm{Da} = \kappa/a^2$ varied in the range of 10^{-6} to 10^{-2}.

At relatively small Reynolds numbers, the flow around a cylinder with a square cross section is comparable with the flow around a circular cylinder: in this connection, it is worth referring to [3, 12]. In [12], a slow viscous flow around an impermeable cylindrical body surrounded by a permeable layer consisting, in turn, of porous cylindrical particles was considered. The character of the flow was analyzed, and the influence of the volume fraction of particles on the product of the Reynolds numbers by the drag of the cylinder was estimated. In [3], issues concerning the ventilation of coats of various animals, which were simulated by a cylindrical permeable layer, were considered. The filtration of fluid in this layer was described by Darcy's equation. Variations in the parameters of the equation made it possible to take into account the diameter and length of hair and wool fiber density.

In the case of large Reynolds numbers ($\mathrm{Re} = 5\times10^3$), the influence of a porous layer on the flow behind a circular cylinder was studied experimentally in [13]. It was shown that the control of the downstream flow is most efficient if the porosity of the layer is 0.4... 0.5, when the Kármán vortex street behind a body does not arise. The passive control of the flow around a semicircular cylinder by means of a porous coating at $\mathrm{Re} = 550$ was considered in [14]. It was noted that a porous layer with a high permeability significantly reduces the aerodynamic drag of the cylinder. For a detached flow around a sphere with a permeable layer at moderate Reynolds numbers, it was established in [15] that, with an increase in the permeability, the detachment point of the flow is displaced downstream. The drag of a sphere is described by the formula

$$C_D = 9.85\,\mathrm{Re}^{-0.5}\,\Delta^{-0.05}(0.025 \le \Delta \le 5),$$

where Δ is a parameter at the ratio of the thickness of the permeable layer to the square root of the permeability.

In all the above-cited works, the flow of the fluid was supposed to be isothermal. The cross-flow around a circular cylinder and its heat exchange with the fluid in the three-dimensional formulation were studied numerically in [4]. A specific feature of the structure under consideration is that a thin permeable layer is found at a certain distance from the impermeable cylinder. In this case, behind the body, a transient regime with periodic detachment of vortices from the surface was observed while the flow between the cylinder and the permeable layer remained laminar.

When studying the flow around and heat exchange with bodies consisting of an impermeable core and a permeable layer, one should take into account the following limiting cases. If the permeability of the layer is fixed while the thickness of the layer tends to zero, the body is impermeable. On the contrary, with an increase in the layer thickness and decrease in the core sizes, we obtain in the limit a fully permeable body, as in the case when the thickness of the porous layer is fixed and its permeability decreases. If the permeability decreases, we obtain an impermeable body but with smaller sizes.

If we consider a nonisothermal cross-flow around a porous permeable square cylinder as a limiting case of the flow around a composite cylinder, it is worth mentioning some more works. Analysis of an isothermal flow of a viscous fluid around such a cylinder has shown [16] that the structure of the flow largely depends on the Reynolds and Darcy numbers and, with increasing Darcy number, i.e., increasing permeability, the drag of the cylinder decreases.

In contrast to [16], in [17], the flow around and heat exchange with a square permeable cylinder were studied under the condition that the surface temperature is constant. The Reynolds number varied from 1 to 40, and the Darcy number, in the interval 10^{-6}–10^{-2}. It was found that, with an increase in the Darcy number, the drag and the length of the vortex region behind the body decrease and the heat transfer increases from the upstream side and decreases on the opposite side. The mean Nusselt number increases with increasing Reynolds and Darcy numbers.

A nonstationary laminar flow around a square cylinder with a heated base and forced convective heat exchange with the flow was studied numerically in [18]. The Reynolds number varied from 50 to 250, the Darcy number varied in the range 10^{-6}–10^{-2}, and the porosity, in the range of 0.4 to 0.8.

In the above-cited works, the fluid was supposed to be homogeneous. However, in nature and engineering, the media are frequently multiphased and contain mechanical additives [19–23], the material of permeable bodies is inhomogeneous [24], and the action upon them may have the character of shock waves [25]. The analysis of the influence of all these factors on the processes under consideration is of significant interest.

The review presented above gives evidence that hydrodynamics and heat transfer of porous bodies, especially high-drag ones, are insufficiently known. There are little or no data on the flow at large Reynolds numbers, including turbulent flows, and flows around bodies with an anisotropic porosity, consisting of regions with different permeability and performing rotational or oscillatory motion, deformed or found in multiphase streams.

The present work is devoted to studying the influence of the permeability of a porous layer covering a cylinder with a square cross section on the hydrodynamic characteristics and heat transfer in a laminar flow of a viscous incompressible fluid.

PROBLEM STATEMENT

We consider a nonisothermal flow of a viscous incompressible fluid around a composite cylinder with a square cross section with an edge length a at moderate Reynolds numbers Re = 1–40. The computational domain is a rectangle of length 0.5 m and width 0.2 m in which, at a distance of 0.1 m from the entry section, at equal distances from the lateral sides, an impermeable core with a square cross section and an edge length b = 0.005 m, surrounded by a porous layer of thickness h = 0.0025 m is placed; in this case, a = 0.01 m (Fig. 1).

In the Cartesian reference frame x_1Ox_2, the origin of which is placed at the center of the cross section of the cylinder and of which the axis Ox_1 is directed downstream, a plane-parallel laminar flow of a viscous incompressible fluid is described by the equations

$$\frac{\partial v_i}{\partial x_i} = 0, \tag{1}$$

$$\frac{1}{\varepsilon}\frac{\partial v_i}{\partial t} + v_j\frac{1}{\varepsilon^2}\frac{\partial v_i}{\partial x_j} = -\frac{1}{\rho}\frac{\partial p}{\partial x_i} + \nu\frac{1}{\varepsilon}\frac{\partial^2 v_i}{\partial x_j \partial x_j} - \frac{\nu}{\kappa}v_i, \quad i = 1,2. \tag{2}$$

Here, t is time, $v_i = \varepsilon u_i$ are the components of the Darcy velocity, u_i are the components of the fluid velocity $\mathbf{u}$, p is pressure, ρ is the density of the fluid, ν is the kinematic viscosity of the fluid, κ is the permeability of the cylinder, and ε is the porosity:

$$\varepsilon = \begin{cases} 1 & \text{outside the cylinder,} \\ 0 < \varepsilon < 1 & \text{in the porous layer;} \end{cases}$$

repeated indices are implicitly summed over.

We assume that the material of the permeable layer has a corpuscular structure; therefore, the porosity ε and permeability κ are coupled by the Cozeny–Carman relationship [26]

$$\kappa = \frac{1}{150}\frac{\varepsilon^3 d_p^2}{(1-\varepsilon)^2},$$

where d_p is the typical particle diameter in the porous layer.

The energy equation for a fluid has the form

$$\frac{\partial}{\partial t}(\rho E) + \nabla(\mathbf{u}(\rho E + p)) = \lambda\Delta T - Q_w. \tag{3}$$

Here, $E = H - \frac{p}{\rho} + \frac{u^2}{2}$, H is the enthalpy, T is temperature, λ is the thermal conductivity of the fluid, and Q_w is the heat flux power in the matrix of the permeable layer [5, 27, 28].

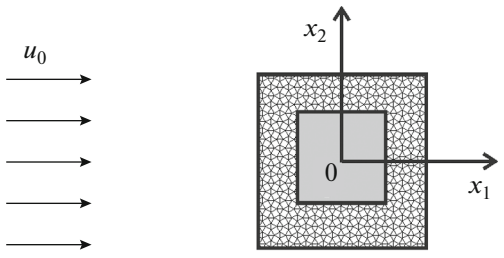

Fig. 1. Schematic of the computational domain.

Boundary and Initial Conditions

In the entry section, perpendicular to the axis Ox_1, we set $u_1 = u_0 = \text{const}$ and $u_2 = 0$; the operating pressure p_0 = 0.1 MPa; and the ambient temperature $T = T_0 = \text{const}$.

At the exit of the computational domain, we impose the "soft" boundary conditions: $\frac{\partial u_1}{\partial x_1} = 0$, $\frac{\partial u_2}{\partial x_1} = 0$, $\frac{\partial p}{\partial x_1} = 0$, and $\frac{\partial T}{\partial x_1} = 0$, which mean the leveling of both hydrodynamic and thermal characteristics of the flow far from the cylinder.

At the lateral sides, we set $\frac{\partial u_1}{\partial x_2} = 0$, $u_2 = 0$, $\frac{\partial p}{\partial x_2} = 0$, and $\frac{\partial T}{\partial x_2} = 0$.

At the surface of the impermeable cylinder, we impose the no-slip conditions $u_1 = u_2 = 0$ and a constant temperature $T = T_w$. In the region of the permeable layer, the porosity ε and permeability κ vary due to the intense heat transfer and high heat conductivity of the material of the matrix and the temperature is $T = T_w$.

At the initial moment of time $t = 0$, the medium begins the motion, $u_1 = u_0$, $u_2 = 0$, $p = p_0$, and $T = T_0$.

The solution of the problem is performed by the finite-volume method on a triangle mesh refined with an approach to the surface of the body by means of ANSYS Fluent software.

RESULTS OF CALCULATION

The parameters of an incompressible fluid (air) are specified as follows: the density ρ = 1.225 kg/m³, the dynamic viscosity $\mu = 1.79\times10^{-5}$ kg/(m s), the specific heat capacity at a constant pressure c = 1000 J/(kg K), and the thermal conductivity λ = 0.0242 W/(m K). The fluid velocity at the exit is $u_0 = \mu\,\mathrm{Re}/a\rho$, and the Reynolds number Re is varied. The temperature at the exit is T_0 = 300 K, and T_w = 350 K.

When calculating the flow of a fluid around a body, the main calculated parameters are the drag

Parameters C_D, L, and $\overline{\mathrm{Nu}}$ for an impermeable cylinder

Re	C_D			L			$\overline{\mathrm{Nu}}$		
	a	*b*	*c*	*a*	*b*	*c*	*a*	*b*	*c*
1	14.44	14.37	14.40	–	–	–	0.714	0.67	0.65
5	4.88	5.007	4.840	0.30	0.313	0.309	1.22	1.18	1.20
10	3.34	3.375	3.390	0.62	0.645	0.65	1.598	1.54	1.58
20	2.397	2.402	2.401	1.30	1.30	1.39	2.093	2.12	2.19
30	2.00	2.014	2.010	2.025	1.98	2.11	2.46	2.37	2.39
40	1.78	1.798	1.767	2.75	2.66	2.82	2.75	2.66	2.62

$C_D = \dfrac{F_{x1}}{0.5\rho u_0^2 a}$ and the Nusselt number $\mathrm{Nu} = a\alpha/\lambda$, which characterizes the intensity of heat transfer. Here, F_{x1} is the projection of the hydrodynamic drag of the cylinder onto the axis Ox_1, $\alpha = \dfrac{\lambda}{T_w - T_0}\left(\dfrac{\partial T}{\partial n}\right)$ is the local convective heat transfer coefficient, and n is the outward normal to the surface of the cylinder.

Preliminarily, the flow around an impermeable square cylinder with an edge length a was calculated. The table presents the values of the drag C_D, the length L of the vortex trail, and the mean Nusselt number $\overline{\mathrm{Nu}}$, obtained in our calculations (*a*) and taken from [17] (*b*) and [29] (*c*). It is seen that the calculated values of C_D, L, and $\overline{\mathrm{Nu}}$ are in a good agreement with the existing.

It was established in the numerical experiments that the flow around a composite square cylinder at Reynolds numbers in the range 1–40, porosity of the layer $\varepsilon = 0.5$, and Darcy numbers $\mathrm{Da} = \kappa/a^2$ in the range $10^{-6} \le \mathrm{Da} \le 10^{-2}$ proceeds in stationary regime. The Kármán vortex street behind the cylinder is not formed. The streamlines in a part of the computational domain for $\mathrm{Re} = 40$ and $\mathrm{Da} = 10^{-2}$ are shown in Fig. 2. In the upper part of the figure, the streamlines of the flow around a composite cylinder with a porous coating are presented and, in the lower part, for comparison, the streamlines of the flow around a fully permeable cylinder. It is seen that, in the case of a cylinder with an impermeable core, a vortex region is formed behind the body and a fraction of it is situated in the permeable layer. Moreover, the flow is detached from the impermeable core rather than from the surface of the permeable layer. The penetration of a recirculation vortex into a porous structure of a circular cylinder was also noted in [30].

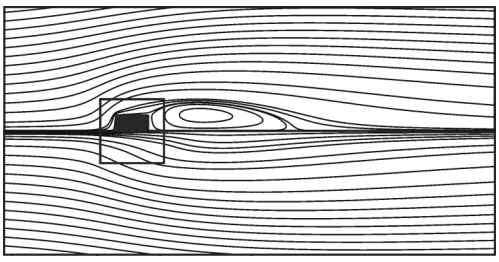

Fig. 2. Streamlines for $\mathrm{Re} = 40$ and $\mathrm{Da} = 10^{-2}$ of (upper part) a cylinder with a permeable layer and (lower part) a permeable cylinder.

At the same values of Re and Da, the velocities v_n against the normal to the front (*A*), lateral (*B*, *D*), and back (*C*) sides are shown in Fig. 3 for two cases: composite (*1*) and permeable (*2*) cylinders. The impermeable core significantly affects the inflow and outflow of fluid at all sides of the cylinder. It is seen that the normal velocity of the fluid at the front side decreases, changes the sign at the rear side, and has a pronounced nonlinear character at the lateral sides.

It should be noted that, for a low permeability of the porous layer ($\mathrm{Da} = 10^{-6}$–10^{-3}), the fluid flows out from the cylinder mainly through its lateral sides. In this case, the maximum variation in the normal velocity at the lateral sides is observed near the front angular points. In this region, the vorticity field significantly changes.

Typical isotherms of the temperature field in the selected part of the computational domain for $\mathrm{Re} = 40$ and $\mathrm{Da} = 10^{-2}$ are presented in Fig. 4. Here, as above, the upper part of the figure shows isotherms of the flow around a cylinder with a permeable layer and lower part show isotherms of the flow around a fully permeable cylinder. The main difference between these cases is that, in the absence of an impermeable core, the heated fluid moves downstream of the cylinder somewhat farther than in the presence of the core.

Analysis of the nature of variation in the Nusselt number in different parts of the surface of the cylinder with a porous layer has shown that the heat transfer is maximal on the front side and minimal on the rear side. However, along the surface of each side, the heat transfer intensity varies significantly, especially in the vicinity of the angular points of the body. With increasing permeability of the layer, the local Nusselt

numbers on the front side appreciably increase but, on the lateral and rear sides, they slightly decrease.

The calculated values of the mean Nusselt number $\overline{\mathrm{Nu}}_f$ on the front side of the cylinder (Fig. 5) practically coincide with the data obtained for a permeable cylinder in [17]. At a high permeability ($\mathrm{Da} = 10^{-2}$) and Reynolds numbers $\mathrm{Re} > 20$, a discrepancy between the results are observed. Moreover, the greater the Reynolds number, the greater the discrepancy. In our opinion, the reason for the discrepancy is that, in [17], only the surface part of the matrix of the cylinder is heated while, in the present work, the whole matrix is heated. In addition, the results of [17] were obtained with allowance for the inertial component in the dependence of the pressure jump during the motion of the fluid through the permeable body, the influence of which is stronger at large Reynolds numbers.

As was noted above, with an increase in the permeability, the heat transfer on the rear side of the cylinder decreases (Fig. 6). If the Darcy numbers are small ($\mathrm{Da} = 10^{-6}, 10^{-4}, 10^{-3}$), then, with an increase in the Reynolds number, the mean Nusselt number $\overline{\mathrm{Nu}}_r$ on this side increases; the most intensive increase is observed for $\mathrm{Re} < 5$. In the interval $5 \le \mathrm{Re} \le 40$, the dependence of $\overline{\mathrm{Nu}}_r$ on Re is close to linear. In the case of relatively large Darcy numbers $\mathrm{Da} = 10^{-2}$, for $\mathrm{Re} \sim 5$, we have a pronounced maximum in the dependence of $\overline{\mathrm{Nu}}_r$ on Re, especially for the permeable cylinder. The increase in the Nusselt number with an increase in the Reynolds number has obvious causes, while the reduction in the heat transfer ($\mathrm{Da} = 10^{-2}$) with an increase in the Reynolds number to $\mathrm{Re} > 5$ needs explanation. It is seen from Fig. 2 (lower part) that the vortex region behind the cylinder is not formed and the velocity of the flow through the cylinder is relatively high in its central part and low in the periphery. In our opinion, the significant nonuniformity of the fluid velocity in the cylinder across the flow may be the reason of such an unusual behavior of the Nusselt number as a function of the incident Reynolds number.

For a relative thickness of the porous layer $\bar{h} = h/a = 0.25$, the dependence of the mean Nusselt number $\overline{\mathrm{Nu}}_b$ at the lateral sides of the cylinder on the Reynolds and Darcy numbers ($7 \le \mathrm{Re} \le 40$, $10^{-6} \le \mathrm{Da} \le 10^{-2}$) can be approximated by the formula

$$\overline{\mathrm{Nu}}_b = 0.45(1 - 0.025\log \mathrm{Da})(1 - 0.008\,\mathrm{Re})\sqrt{\mathrm{Re}}.$$

Practically the same dependence $\overline{\mathrm{Nu}}_b(\mathrm{Re}, \mathrm{Da})$ is observed for a permeable cylinder.

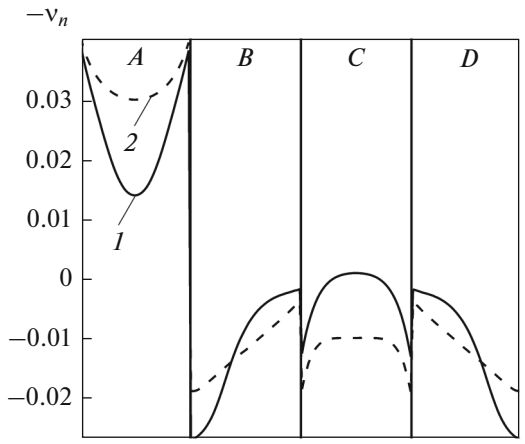

Fig. 3. Fluid velocity against the normal to the surface of the cylinder for $\mathrm{Re} = 40$ and $\mathrm{Da} = 10^{-2}$: (*1*) a cylinder with a permeable layer and (*2*) a permeable cylinder.

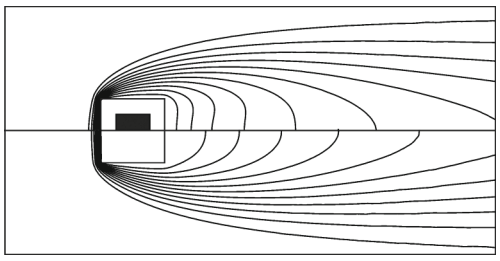

Fig. 4. Isotherms of a flow with $\mathrm{Re} = 40$ and $\mathrm{Da} = 10^{-2}$ around (upper part) a cylinder with a permeable layer and (lower part) a permeable cylinder.

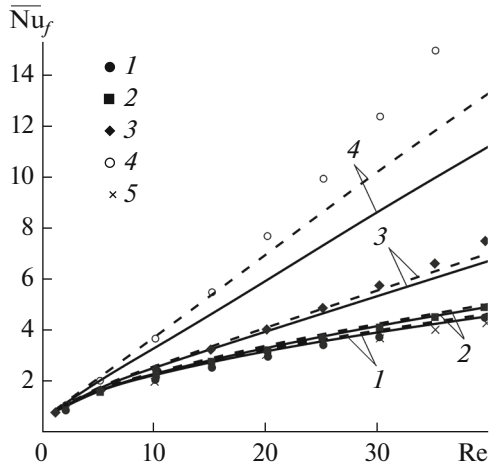

Fig. 5. Mean Nusselt number, $\overline{\mathrm{Nu}}_f$, on the front side of the surface of the cylinder for $\mathrm{Re} = 40$ and $\mathrm{Da} = 10^{-6}$ (*1*), (*2*) 10^{-4}, (*3*) 10^{-3}, and (*4*) 10^{-2}; the flow around (solid curve) a cylinder with a permeable layer and (dashed line) a permeable cylinder; (*1–4*) comparison with the data of [17]; (*5*) an impermeable cylinder.

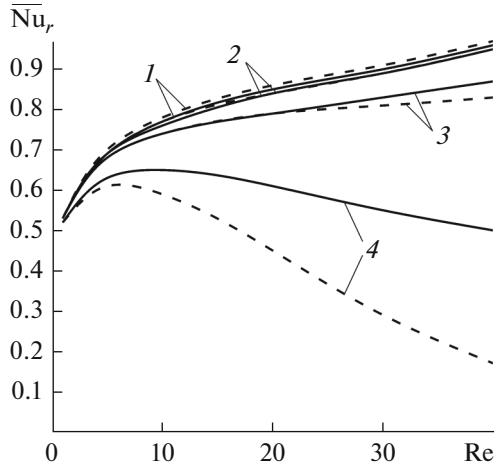

Fig. 6. Mean Nusselt number, $\overline{\mathrm{Nu}}_r$, on the rear side of the surface of the cylinder for Re = 40 and Da = 10^{-6} (*1*), (*2*) 10^{-4}, (*3*) 10^{-3}, and (*4*) 10^{-2}; the flow around (solid curve) a cylinder with a permeable layer and (dashed line) a permeable cylinder.

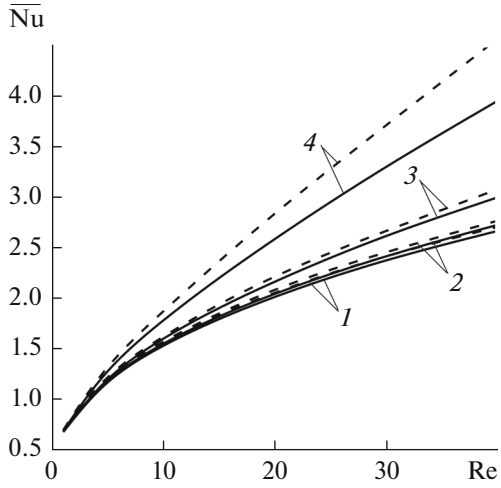

Fig. 7. Mean Nusselt number, $\overline{\mathrm{Nu}}_f$, over the entire surface of the cylinder for Re = 40 and Da = 10^{-6} (*1*), (*2*) 10^{-4}, (*3*) 10^{-3}, and (*4*) 10^{-2}; the flow around (solid curve) a cylinder with a permeable layer and (dashed line) a permeable cylinder.

With an increase in the Reynolds and Darcy numbers in the aforementioned ranges, the mean Nusselt number over the entire surface of the cylinder, $\overline{\mathrm{Nu}}$, increases almost linearly by the formula

$$\overline{\mathrm{Nu}} = 1.25 + 0.13\left(0.9 - 0.14\left(-\log \mathrm{Da}\right)^{0.8}\right)\left(\mathrm{Re} - 5\right).$$

It should be noted that, in general, the heat transfer on the surface of the cylinder in the presence of an impermeable core is smaller than in its absence (Fig. 7).

CONCLUSIONS

The calculations of the cross-flow of a viscous incompressible fluid around a porous cylindrical body with a square cross section at moderate Reynolds numbers have shown that the structure of the body and the permeability of the porous material have a substantial effect on the character of the flow and the heat transfer. The maximum heat transfer is observed on the front side in the vicinity of the angles of the cylinder. According to our calculations, for Reynolds numbers Re > 5, the dependence of the mean Nusselt number on the Reynolds number in the flow around composite and homogeneous permeable cylinders is close to linear. With an increase in the Darcy number, the heat transfer from the porous cylinders under consideration increase in proportion to $\left(-\log \mathrm{Da}\right)^{0.8}$. Thus, application of permeable layers onto streamlined bodies is an efficient way to intensify the heat transfer.

REFERENCES

1. Villee, C.A. and Dethier, V.G., *Biological Principles and Processes*, Philadelphia: W.B. Saunders, 1971.
2. Grzimek, B., *Auf den Mensch gekommen: Erfahrungen mit Leuten*, Berlin: Bertelsmann, 1974.
3. Budaraju, S., Stewart, W.E., and Porter, W.P., *Proc. R. Soc. London, Ser. B*, 1994, no. 256, p. 41.
4. Sobera, M.P. and Kleijn, C.R., *Flow, Turbul. Combust.*, 2008, no. 80, p. 531.
5. Popov, I.A., *Gidrodinamika i teploobmen v poristykh teploobmennykh elementakh i apparatakh. Intensifikatsiya teploobmena* (Hydrodynamics and Heat Transfer in Porous Heat Exchange Elements and Apparatus: Intensification of Heat Transfer), Kazan': Tsentr Innov. Tekhnol., 2007.
6. Faktorovich, L.M., *Kratkii spravochnik po teplovoi izolyatsii* (Brief Reference Book on Thermal Insulation), Leningrad: Gostekhizdat, 1962.
7. Bogoslovskii, V.N., *Stroitel'naya teplofizika* (Thermophysics for Building), St. Petersburg: AVOK Severo-Zapad, 2006.
8. *Teplotekhnika* (Heat Engineering), Lukanin, V.N., Ed., Moscow: Vysshaya Shkola, 2000.
9. Kutateladze, S.S., *Teploperedacha i gidrodinamicheskoe soprotivlenie. Spravochnoe posobie* (Heat Transfer and Hydrodynamic Resistance: Handbook), Moscow: Energoatomizdat, 1990.
10. Bolgarskii, A.V., Mukhachev, G.A., and Shchukin, V.K., *Termodinamika i teploperedacha. Uchebnik dlya VUZov* (Thermodynamics and Heat Transfer: Textbook for High Schools), Moscow: Vysshaya shkola, 1975.
11. Rong, F.M., Guo, Z.L., Lu, J.H., and Shi, B.C., *Int. J. Numer. Methods Fluids*, 2011, vol. 65, no. 10, p. 1217.
12. Deo, S., Yadav, P.K., and Tiwari, A., *Appl. Mathem. Modell.*, 2010, no. 34, p. 1329.
13. Gozmen, B., Firat, E., Akilli, H., and Sahin, B., *EPJ Web Conf.*, 2013, vol. 45, 01035. doi 10.1051/epjconf/20134501035
14. Mimeau, C., Mortazavi, I., and Cottet, G.-H., *Int. J. Flow Control*, 2014, vol. 6, no. 1, p. 43.

15. Taamneh, Y. and Bataineh, K.M., *Transp. Porous Media*, 2011, vol. 90, no. 3, p. 869.
16. Jue, T., *Int. J. Numer. Methods Heat Fluid Flow*, 2004, vol. 14, no. 5, p. 649.
17. Dhinakaran, S. and Ponmozhi, J., *Energy Convers. Manage*, 2011, no. 52, p. 2170.
18. Perng, S.W., Wu, H.W., Wang, R.H., and Jue, T.C., *Int. J. Therm. Sci.*, 2011, no. 50, p. 2006.
19. Nigmatulin, R.I., *Dinamika mnogofaznykh sred* (Dynamics of Multiphase Media), Moscow: Nauka, 1987, ch. 1.
20. Zeigarnik, Yu.A. and Polyaev, V.M., *J. Eng. Phys. Thermophys.*, 2000, vol. 73, no. 6, p. 1093.
21. Grigor'eva, O.V. and Zaripov, Sh.Kh., *Russ. Aeronaut. (Iz VUZ)*, 2012, vol. 55, no. 1, p. 19.
22. Laptev, A.G. and Farakhov, M.I., *Khim. Prom-st'*, 2008, vol. 85, no. 3, p. 156.
23. Morenko, I.V. and Fedyaev, V.L., *J. Eng. Phys. Thermophys.*, 2014, vol. 87, no. 3, p. 566.
24. Epov, M.I., Terekhov, V.I., Nizovtsev, M.I., Shurina, E.P., Itkina, N.B., Ukolov, E.S., *High Temp.*, 2015, vol. 53, no. 1, p. 45.
25. Mirova, O.A., Kotel'nikov, A.L., Golub, V.V., and Bazhenova, T.V., *High Temp.*, 2015, vol. 53, no. 1, p. 155.
26. Rashidi, S., Bovand, M., Pop, I., and Valipour, M.S., *Transp. Porous Media*, 2014, no. 102, p. 207.
27. Zeigarnik, Yu.A. and Ivanov, F.P., *High Temp.*, 2010, vol. 48, no. 3, p. 382.
28. Direktor, L.B., Zaichenko, V.M., Maikov, I.L., Kosov, V.F., Sinel'shchikov, V.A. and Torchinskii, V.M., *High Temp.*, 2010, vol. 48, no. 6, p. 887.
29. Sharma, A. and Eswaran, V., *Numer. Heat Transfer, Part A*, 2004, no. 45, p. 247.
30. Yu, P., Zeng, Y., Lee, T.S., Chen, X.B., and Low, H.T., *Comput. Fluids*, 2011, no. 42, p. 1.

Translated by E. Chernokozhin